Electronic Supplementary Material (ESI) for Inorganic Chemistry Frontiers.

ESI-TOF MS analysis and DNA cleavage activity of rutin-metal complexes in aqueous extracts of medicinal plants

Weilan Cai[a], Kangkang Zheng[a], Zhimin Li[a]*, Liang Peng[a]*, Qianrong Yin[a], and Haijun Zeng[a]

[a]*Engineering Center of Jiangxi University for Fine Chemicals, School of Pharmacy, Jiangxi Science & Technology Normal University, Nanchang 330013, PR China.*

**Corresponding authors*

Table of Contents

Content	Page No.
Supplementary Table S1. HPLC results for the reaction products of rutin and eight metal ions in hot water dissolved in 15 % formic acid-methanol and methanol	**4**
Supplementary Fig. S1. HPLC spectra of the aqueous Violae Herba extract dissolved in (A) 15 % formic acid-methanol and (B) methanol.	**5**
Supplementary Table S2. HPLC results for the aqueous Violae Herba extracts dissolved in 15 % formic acid-methanol and methanol	**5**
Supplementary Fig. S2. HPLC spectra of the aqueous Lonicerae Japonicae Flos extract dissolved in (A) 15 % formic acid-methanol and (B) methanol.	**6**
Supplementary Table S3. HPLC results for the aqueous Lonicerae Japonicae Flos extracts dissolved in 15 % formic acid-methanol and methanol	**6**
Supplementary Fig. S3. HPLC spectra of the aqueous Forsythiae Fructus extract dissolved in (A) 15 % formic acid-methanol and (B) methanol.	**7**
Supplementary Table S4. HPLC results for the aqueous Forsythiae Fructus extracts dissolved in 15 % formic acid-methanol and methanol	**7**
Supplementary Fig. S4. UV–Vis spectra of reaction liquids: rutin-Ca^{2+} (A), rutin-Mg^{2+} (B), rutin-Zn^{2+} (C), rutin-Fe^{3+} (D), rutin-Ni^{2+} (E), rutin-Mn^{2+} (F), rutin-Sr^{2+} (G)	**8**
Supplementary Fig. S5-1. Theoretical isotopic distribution (a) and measured isotopic distribution (b) of $C_{27}H_{29}O_{16}Ca$	**9**
Supplementary Fig. S5-2. Theoretical isotopic distribution (a) and measured isotopic distribution (b) of $C_{54}H_{59}O_{32}Ca$	**9**
Supplementary Fig. S5-3. Theoretical isotopic distribution (a) and measured isotopic distribution (b) of $C_{54}H_{57}O_{32}Ca_2$	**9**
Supplementary Fig. S5-4. Theoretical isotopic distribution (a) and measured isotopic distribution (b) of $C_{81}H_{89}O_{48}Ca$	**10**
Supplementary Fig. S6-1. Theoretical isotopic distribution (a) and measured isotopic distribution (b) of $C_{27}H_{29}O_{16}Zn$	**11**
Supplementary Fig. S6-2. Theoretical isotopic distribution (a) and measured isotopic distribution (b) of $C_{54}H_{59}O_{32}Zn$	**11**
Supplementary Fig. S6-3. Theoretical isotopic distribution (a) and measured isotopic distribution (b) of $C_{54}H_{57}O_{32}Zn_2$	**11**
Supplementary Fig. S6-4. Theoretical isotopic distribution (a) and measured isotopic distribution (b) of $C_{81}H_{89}O_{48}Zn$	**12**
Supplementary Fig. S6-5. Theoretical isotopic distribution (a) and measured isotopic distribution (b) of $C_{81}H_{87}O_{48}Zn_2$	**12**
Supplementary Fig. S7-1. Theoretical isotopic distribution (a) and measured isotopic distribution (b) of $C_{27}H_{29}O_{16}Cu$	**13**
Supplementary Fig. S7-2. Theoretical isotopic distribution (a) and measured isotopic distribution (b) of $C_{54}H_{59}O_{32}Cu$	**13**
Supplementary Fig. S7-3. Theoretical isotopic distribution (a) and measured	**13**

isotopic distribution (b) of $C_{54}H_{57}O_{32}Cu_2$	
Supplementary Fig. S7-4. Theoretical isotopic distribution (a) and measured isotopic distribution (b) of $C_{81}H_{89}O_{48}Cu$	**14**
Supplementary Fig. S7-5. Theoretical isotopic distribution (a) and measured isotopic distribution (b) of C81H87O48Cu2	**14**
Supplementary Fig. S8-1. Theoretical isotopic distribution (a) and measured isotopic distribution (b) of $C_{27}H_{29}O_{16}Ni$	**15**
Supplementary Fig. S8-2. Theoretical isotopic distribution (a) and measured isotopic distribution (b) of $C_{27}H_{27}O_{16}Ni_2$	**15**
Supplementary Fig. S8-3. Theoretical isotopic distribution (a) and measured isotopic distribution (b) of $C_{54}H_{59}O_{32}Ni$	**15**
Supplementary Fig. S8-4. Theoretical isotopic distribution (a) and measured isotopic distribution (b) of $C_{54}H_{57}O_{32}Ni_2$	**16**
Supplementary Fig. S8-5. Theoretical isotopic distribution (a) and measured isotopic distribution (b) of $C_{81}H_{89}O_{48}Ni$	**16**
Supplementary Fig. S8-6. Theoretical isotopic distribution (a) and measured isotopic distribution (b) of $C_{81}H_{87}O_{48}Ni_2$	**16**
Supplementary Fig. S9-1. Theoretical isotopic distribution (a) and measured isotopic distribution (b) of $C_{27}H_{29}O_{16}Mn$	**17**
Supplementary Fig. S9-2. Theoretical isotopic distribution (a) and measured isotopic distribution (b) of $C_{27}H_{27}O_{16}Mn_2$	**17**
Supplementary Fig. S9-3. Theoretical isotopic distribution (a) and measured isotopic distribution (b) of $C_{54}H_{59}O_{32}Mn$	**17**
Supplementary Fig. S9-4. Theoretical isotopic distribution (a) and measured isotopic distribution (b) of $C_{54}H_{57}O_{32}Mn_2$	**18**
Supplementary Fig. S9-5. Theoretical isotopic distribution (a) and measured isotopic distribution (b) of $C_{81}H_{89}O_{48}Mn$	**18**
Supplementary Fig. S9-6. Theoretical isotopic distribution (a) and measured isotopic distribution (b) of $C_{81}H_{87}O_{48}Mn_2$	**18**
Supplementary Fig. S10-1. Theoretical isotopic distribution (a) and measured isotopic distribution (b) of $C_{27}H_{29}O_{16}Sr$	**19**
Supplementary Fig. S10-2. Theoretical isotopic distribution (a) and measured isotopic distribution (b) of $C_{54}H_{59}O_{32}Sr$	**19**
Supplementary Fig. S10-3. Theoretical isotopic distribution (a) and measured isotopic distribution (b) of $C_{81}H_{89}O_{48}Sr$	**19**
Supplementary Fig. S11-1. Theoretical isotopic distribution of $C_{54}H_{58}O_{32}Fe$（III）(a) and theoretical isotopic distribution (b) and measured theoretical isotopic distribution (c) of $C_{54}H_{59}O_{32}Fe$（II）	**20**
Supplementary Fig. S11-2. Theoretical isotopic distribution of $C_{81}H_{88}O_{48}Fe$（III）(a) and theoretical isotopic distribution (b) and measured theoretical isotopic distribution (c) of $C_{81}H_{89}O_{48}Fe$（II）	**20**
Supplementary Table S5. Contents of eight trace elements in aqueous extracts of four medicinal plants and that dissolved in 15 % formic acid-methanol or methanol (μg/g)	**21-22**

Supplementary Table S1. HPLC results for the reaction products of rutin and eight metal ions in hot water dissolved in 15 % formic acid-methanol and methanol

	15 % Formic acid-methanol		Methanol	
	Dissolve situation	Peak area	Dissolve situation	Peak area
Rutin	Completely dissolved	1324.77±46.23	Completely dissolved	1341.18±48.65
Rutin+Ca^{2+}	Completely dissolved	1211.31±58.56	Yellow precipitate	674.07±30.44
Rutin+Mg^{2+}	Completely dissolved	1245.31±52.26	Yellow precipitate	953.21±47. 01
Rutin+Zn^{2+}	Completely dissolved	1266.04±55.30	Yellow precipitate	1202.22±66.72
Rutin+Fe^{3+}	Completely dissolved	953.48±49.67	Black precipitate	336.43±20.18
Rutin+Cu^{2+}	Completely dissolved	809.95±39.49	Brown precipitate	589.95±30.397
Rutin+Ni^{2+}	Completely dissolved	1285.68±60.28	Yellow precipitate	1051.02±49.06
Rutin+Mn^{2+}	Completely dissolved	1321.89±56.09	Yellow precipitate	1082.83±54.97
Rutin+Sr^{2+}	Completely dissolved	1299.47±71.96	Yellow precipitate	505.85±22.35

Rutin (0.02 mmol) was separately added to 0.01 mmol of anhydrous calcium chloride, anhydrous zinc chloride, magnesium chloride hexahydrate, iron(III) chloride hexahydrate, copper(II) chloride dihydrate, nickel(II) chloride hexahydrate, manganese(II) chloride tetrahydrate, and strontium chloride hexahydrate in round-bottom flasks. After the addition of 20 mL of distilled water, the contents of the flask were mixed thoroughly by shaking and refluxed at 100 °C with magnetic stirrers for 3 h. The resultant reaction liquids were concentrated to dryness under vacuum, washed multiple times with distilled water at 4 °C for the removal of unreacted metal ions, dried under vacuum, and dissolved in 10 mL 15 % formic acid-methanol or methanol under ultrasound. After dilution 12 times with a solvent that dissolved the sample, the solution was filtered through a 0.22 µm membrane, and finally analyzed by HPLC. An equivalent amount of rutin was subjected to the same procedure and analyzed by HPLC. The samples were analyzed by HPLC under the following conditions: Agilent Eclipse XDB-C18 column (4.6 × 250 mm, 5 µm); detection wavelength: 358 nm; column temperature: 30 °C; flow rate: 1.0 mL/min; injection volume: 10 µL; mobile phase A: 0.1 % formic acid-water; mobile phase B: methanol; elution conditions: 55 % B. Three parallel experiments were performed.

Results indicated that the rutin-metal complexes cannot completely dissolve in methanol, and dissolution in an equivalent volume of 15 % formic acid-methanol solution led to decomposition of the complexes into rutin, ultimately resulting in their complete dissolution.

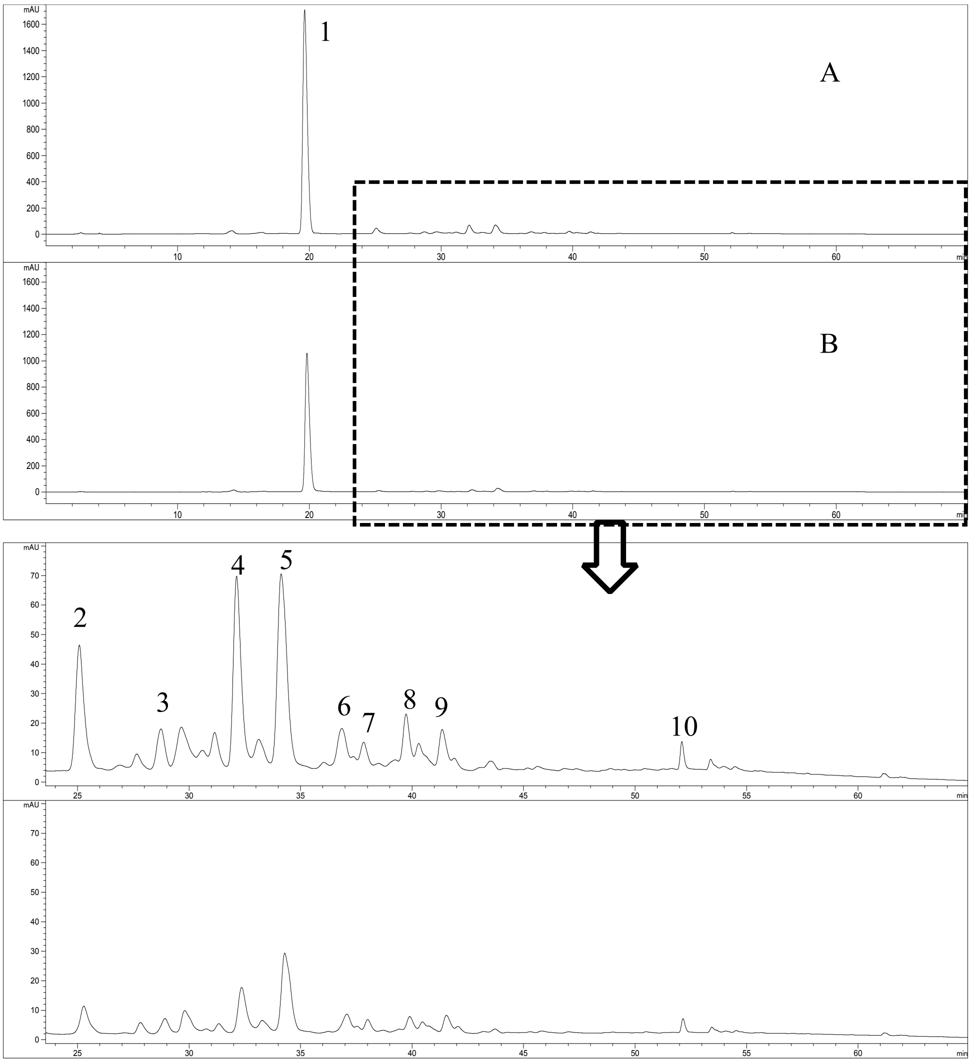

Supplementary Fig. S1. HPLC spectra of the aqueous Violae Herba extract dissolved in (A) 15 % formic acid-methanol and (B) methanol.

Supplementary Table S2. HPLC results for the aqueous Violae Herba extracts dissolved in 15 % formic acid-methanol and methanol

Chromatographic peak number	15 % Formic acid-methanol		Methanol		Increase in peak area (%)
	Retention time/min	Peak area	Retention time/min	Peak area	
1	19.65±0.38	40638.6±2221.09	19.82±0.38	24842.4±987.39	63.59
2	25.08±0.51	1168.58±91.47	25.28±0.50	262.81±17.03	344.65
3	28.74±0.56	313.75±22.08	28.92±0.56	113.62±6.09	176.14
4	32.14±0.64	1594.35±126.53	32.36±0.62	358.97±24.726	344.15
5	34.13±0.67	1993.72±151.44	34.29±0.69	760.66±49.85	162.10
6	36.86±0.77	268.98±14.47	37.073±0.74	111.75±6.94	140.70
7	37.83±0.75	123.86±9.88	38.01±0.75	62.16±3.07	99.26
8	39.73±0.78	419.58±23.52	39.9±0.78	76±5.08	452.08
9	41.35 ± 0.74 (rutin)	280.82 ± 16.01	41.54 ± 0.82	93.46 ± 5.94	200.47
10	52.10±1.02	115.31±2.41	52.15±1.14	57.71±2.18	99.81

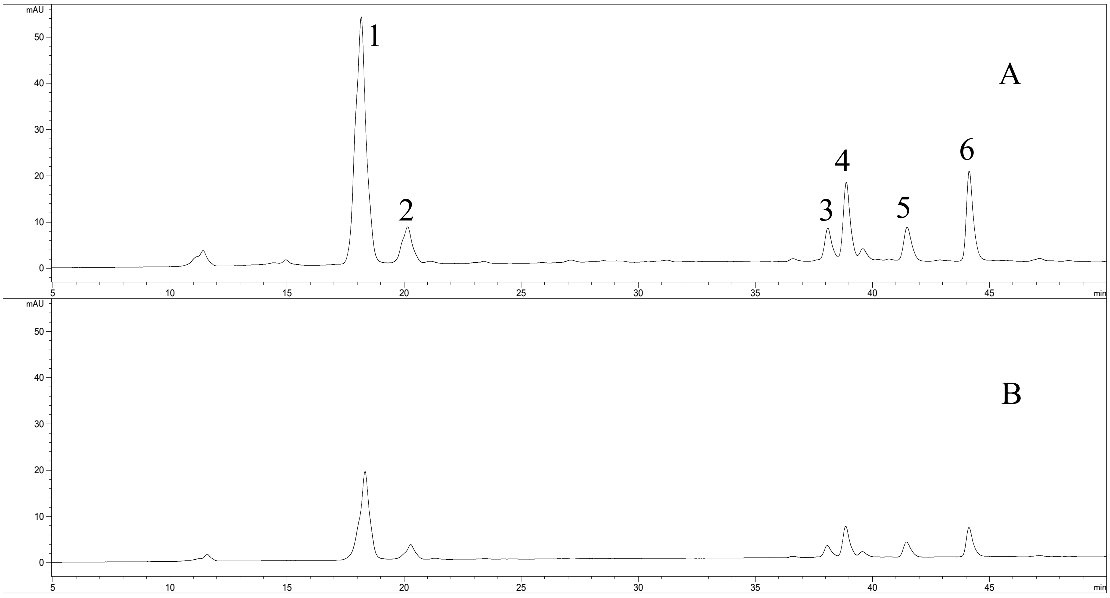

Supplementary Fig. S2. HPLC spectra of the aqueous Lonicerae Japonicae Flos extract dissolved in (A) 15 % formic acid-methanol and (B) methanol.

Supplementary Table S3. HPLC results for the aqueous Lonicerae Japonicae Flos extracts dissolved in 15 % formic acid-methanol and methanol

Chromatographic peak number	15 % Formic acid-methanol		Methanol		Increase in peak area (%)
	Retention time/min	Peak area	Retention time/min	Peak area	
1	18.17±0.34	1727.99±138.24	18.33±0.36	405.37±32.40	201.10
2	20.15±0.42	236.70±18.93	20.28±0.41	573.88±45.87	161.78
3	38.10±0.77	159.43±12.75	38.08±0.76	90.42±7.13	237.06
4	38.88±0.75	365.14±29.18	38.86±0.77	47.3±3.74	197.71
5	41.48 ± 0.82 (rutin)	170.95 ± 9.15	41.46 ± 0.83	75.81 ± 6.41	125.50
6	44.13±0.89	405.37±32.40	44.13±0.89	131.39±10.5112	204.62

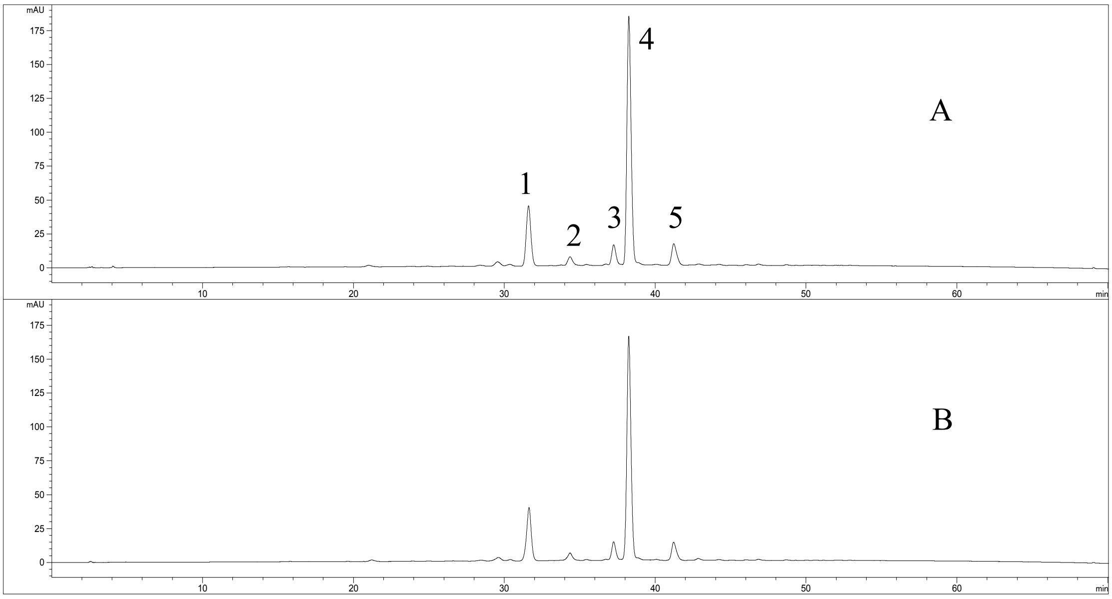

Supplementary Fig. S3. HPLC spectra of the aqueous Forsythiae Fructus extract dissolved in (A) 15 % formic acid-methanol and (B) methanol.

Supplementary Table S4. HPLC results for the aqueous Forsythiae Fructus extracts dissolved in 15 % formic acid-methanol and methanol

Chromatographic peak number	15 % Formic acid-methanol		Methanol		Increase in peak area (%)
	Retention time/min	Peak area	Retention time/min	Peak area	
1	31.60±0.63	960.05±46.80	31.64±0.63	858.26±39.66	11.86
2	34.36±0.67	144.07±8.53	34.36±0.67	119.02±5.82	21.05
3	37.25±0.74	285.01±17.80	37.25±0.75	240.48±12.24	18.52
4	38.25±0.76	3564.74±155.18	38.25±0.78	3069.16±115.52	16.15
5	41.23 ± 0.83	379.06 ± 20.96	41.22 ± 0.82	303.72 ± 22.38	24.81

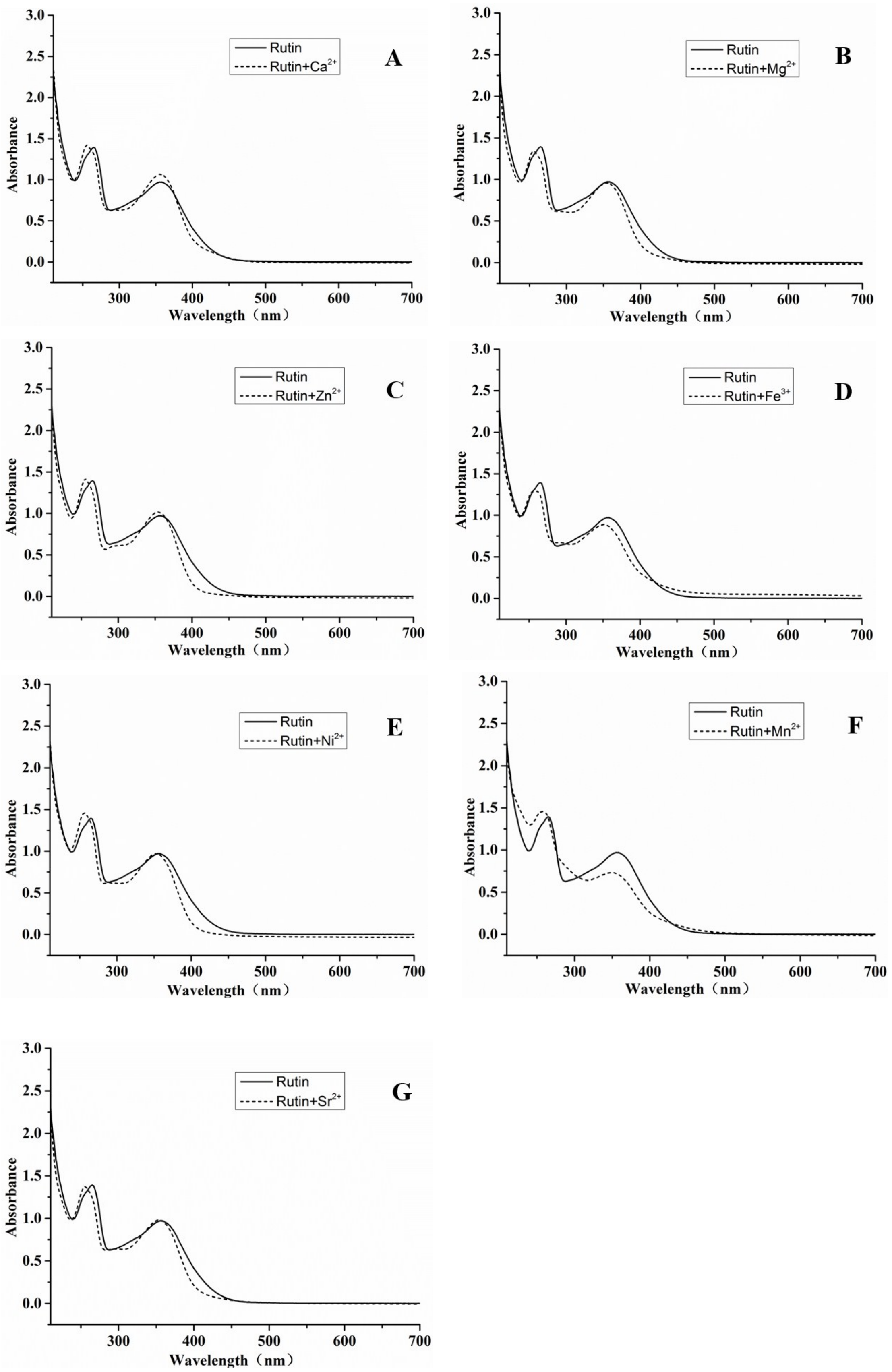

Supplementary Fig. S4. UV–Vis spectra of reaction liquids: rutin-Ca^{2+} (A), rutin-Mg^{2+} (B), rutin-Zn^{2+} (C), rutin-Fe^{3+} (D), rutin-Ni^{2+} (E), rutin-Mn^{2+} (F), rutin-Sr^{2+} (G)

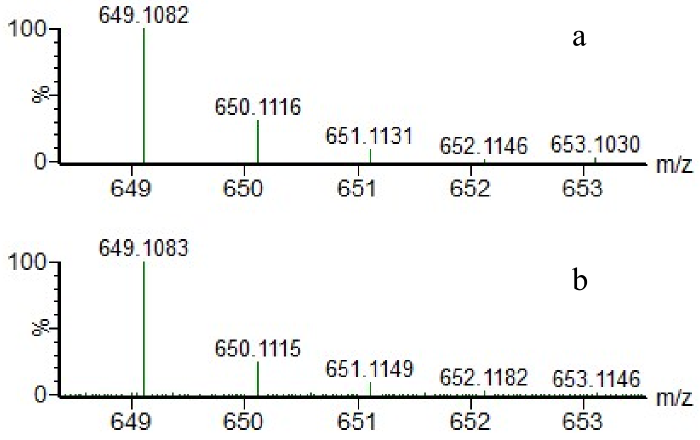

Supplementary Fig. S5-1. Theoretical isotopic distribution (a) and measured isotopic distribution (b) of $C_{27}H_{29}O_{16}Ca$

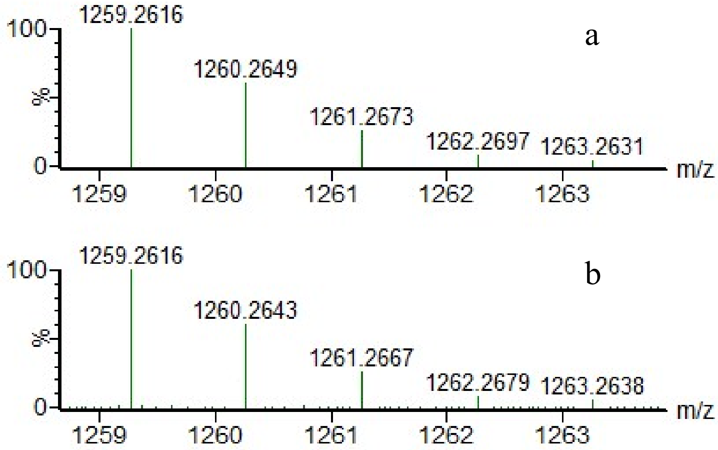

Supplementary Fig. S5-2. Theoretical isotopic distribution (a) and measured isotopic distribution (b) of $C_{54}H_{59}O_{32}Ca$

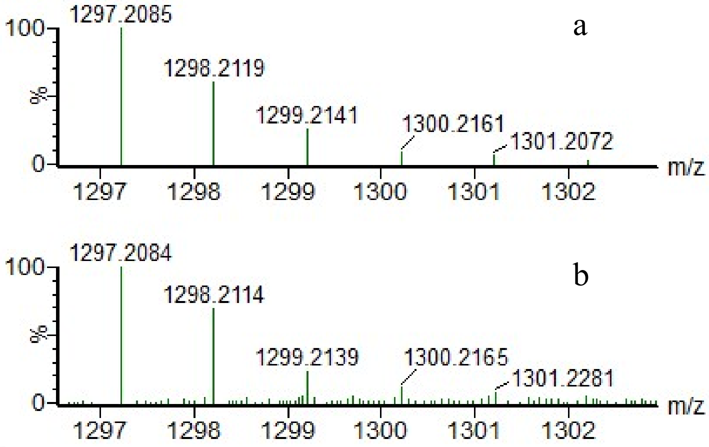

Supplementary Fig. S5-3. Theoretical isotopic distribution (a) and measured isotopic distribution (b) of $C_{54}H_{57}O_{32}Ca_2$

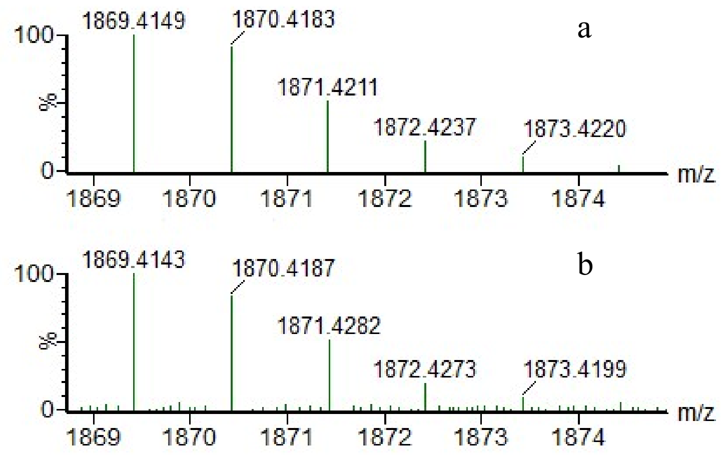

Supplementary Fig. S5-4. Theoretical isotopic distribution (a) and measured isotopic distribution (b) of $C_{81}H_{89}O_{48}Ca$

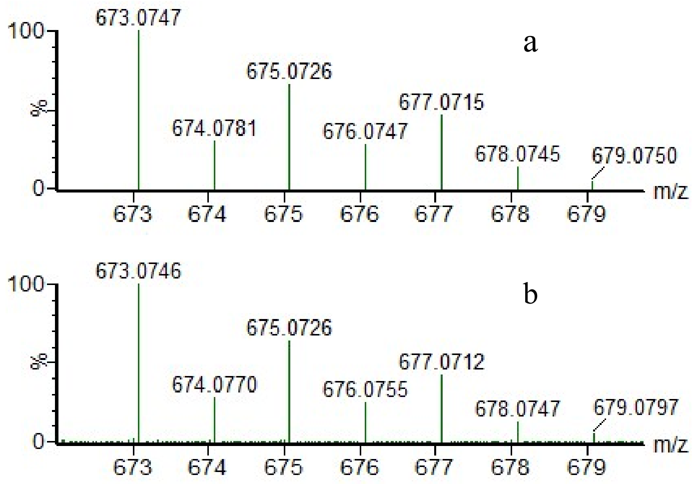

Supplementary Fig. S6-1. Theoretical isotopic distribution (a) and measured isotopic distribution (b) of $C_{27}H_{29}O_{16}Zn$

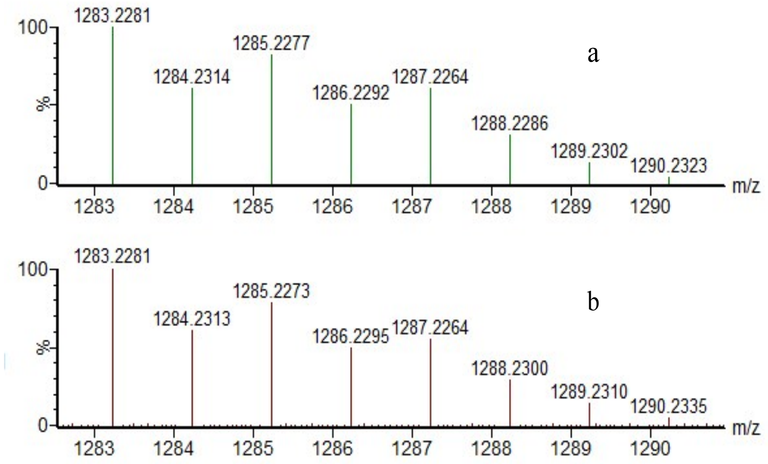

Supplementary Fig. S6-2. Theoretical isotopic distribution (a) and measured isotopic distribution (b) of $C_{54}H_{59}O_{32}Zn$

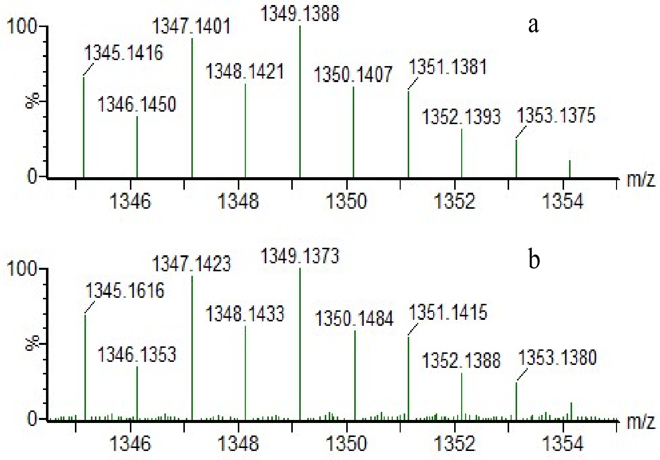

Supplementary Fig. S6-3. Theoretical isotopic distribution (a) and measured isotopic distribution (b) of $C_{54}H_{57}O_{32}Zn_2$

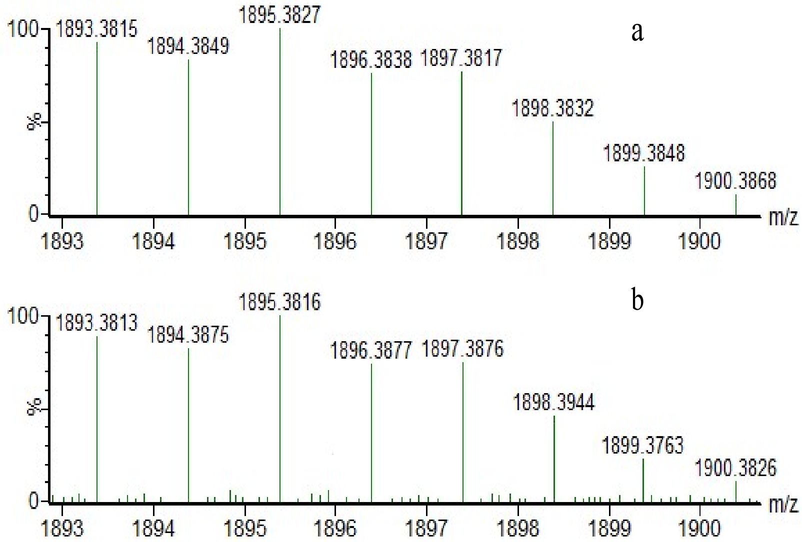

Supplementary Fig. S6-4. Theoretical isotopic distribution (a) and measured isotopic distribution (b) of $C_{81}H_{89}O_{48}Zn$

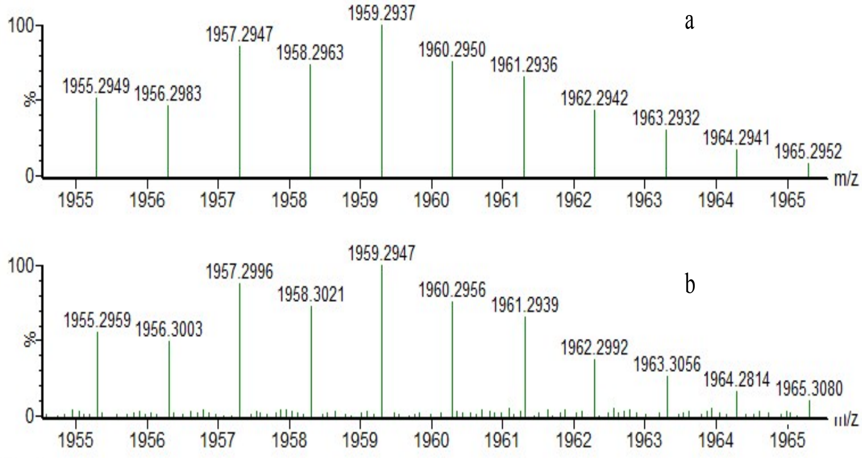

Supplementary Fig. S6-5. Theoretical isotopic distribution (a) and measured isotopic distribution (b) of $C_{81}H_{87}O_{48}Zn_2$

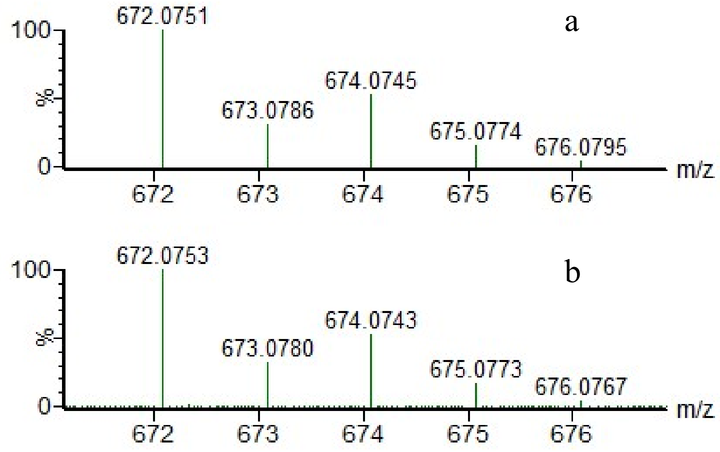

Supplementary Fig. S7-1. Theoretical isotopic distribution (a) and measured isotopic distribution (b) of $C_{27}H_{29}O_{16}Cu$

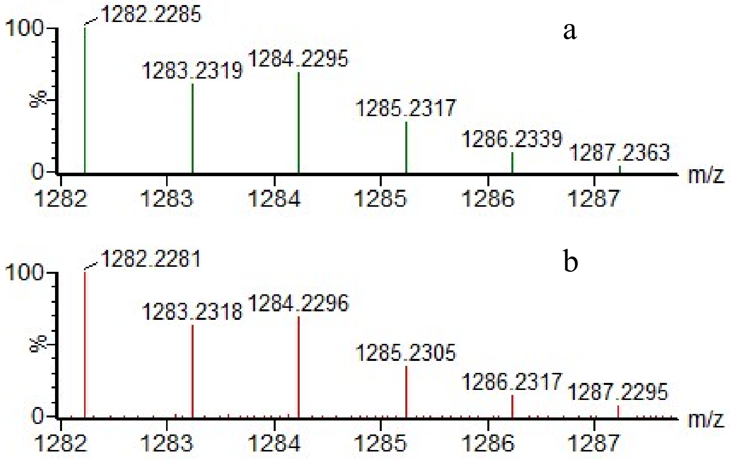

Supplementary Fig. S7-2. Theoretical isotopic distribution (a) and measured isotopic distribution (b) of $C_{54}H_{59}O_{32}Cu$

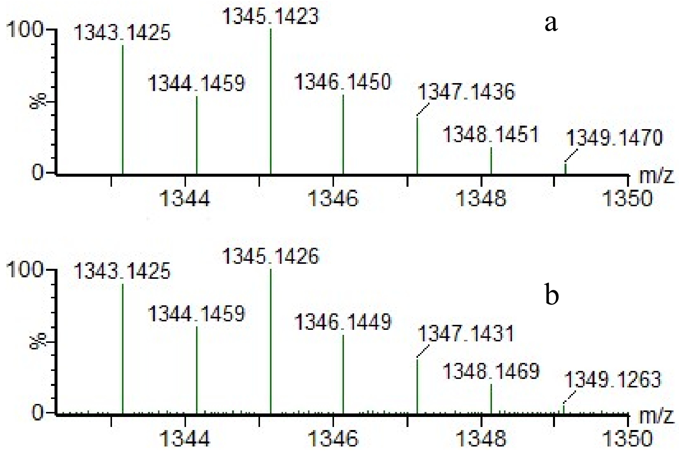

Supplementary Fig. S7-3. Theoretical isotopic distribution (a) and measured isotopic distribution (b) of $C_{54}H_{57}O_{32}Cu_2$

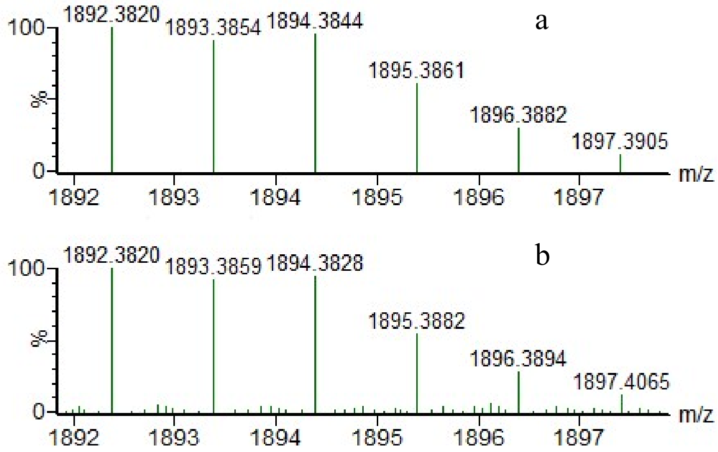

Supplementary Fig. S7-4. Theoretical isotopic distribution (a) and measured isotopic distribution (b) of $C_{81}H_{89}O_{48}Cu$

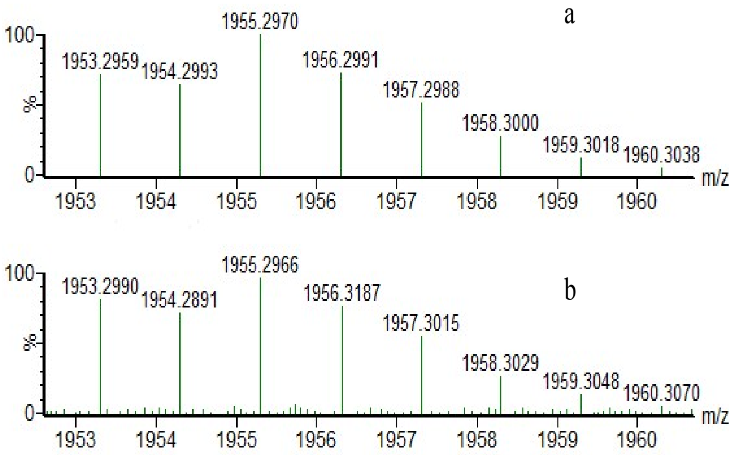

Supplementary Fig. S7-5. Theoretical isotopic distribution (a) and measured isotopic distribution (b) of $C_{81}H_{87}O_{48}Cu_2$

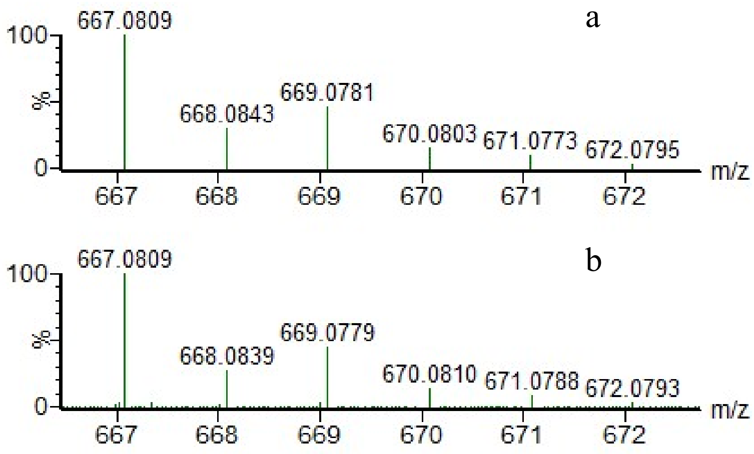

Supplementary Fig. S8-1. Theoretical isotopic distribution (a) and measured isotopic distribution (b) of $C_{27}H_{29}O_{16}Ni$

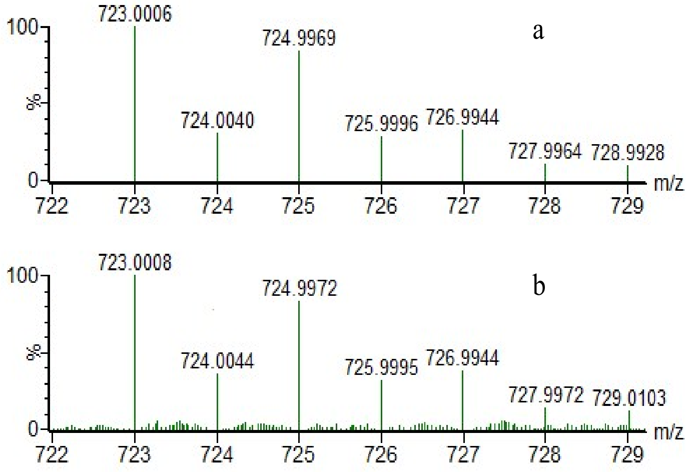

Supplementary Fig. S8-2. Theoretical isotopic distribution (a) and measured isotopic distribution (b) of $C_{27}H_{27}O_{16}Ni_2$

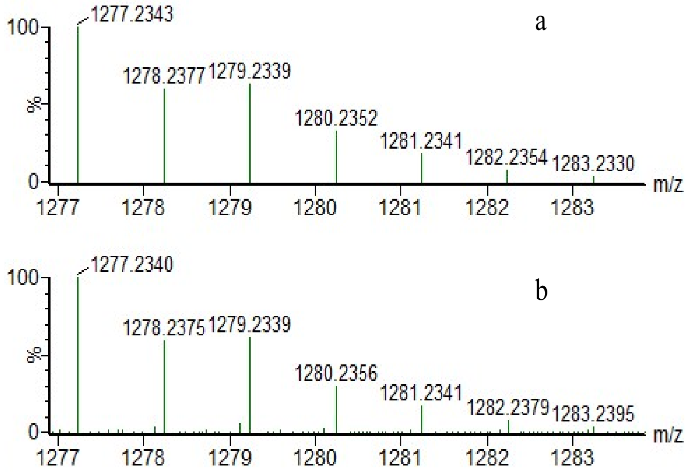

Supplementary Fig. S8-3. Theoretical isotopic distribution (a) and measured isotopic distribution (b) of $C_{54}H_{59}O_{32}Ni$

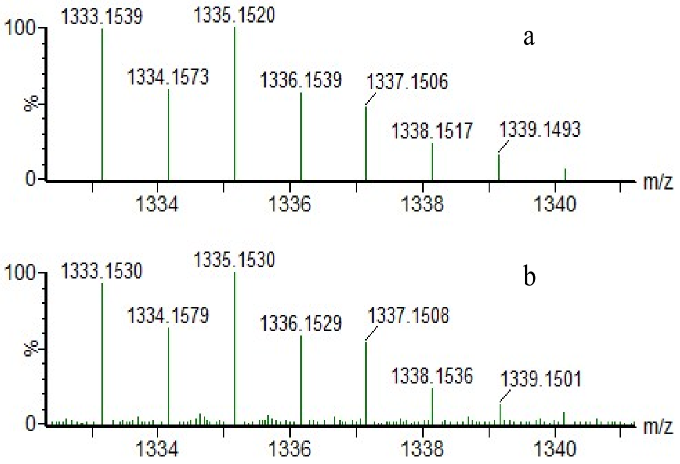

Supplementary Fig. S8-4. Theoretical isotopic distribution (a) and measured isotopic distribution (b) of $C_{54}H_{57}O_{32}Ni_2$

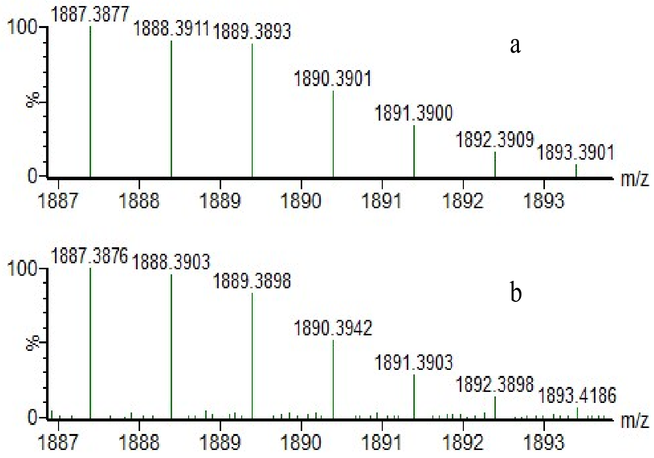

Supplementary Fig. S8-5. Theoretical isotopic distribution (a) and measured isotopic distribution (b) of $C_{81}H_{89}O_{48}Ni$

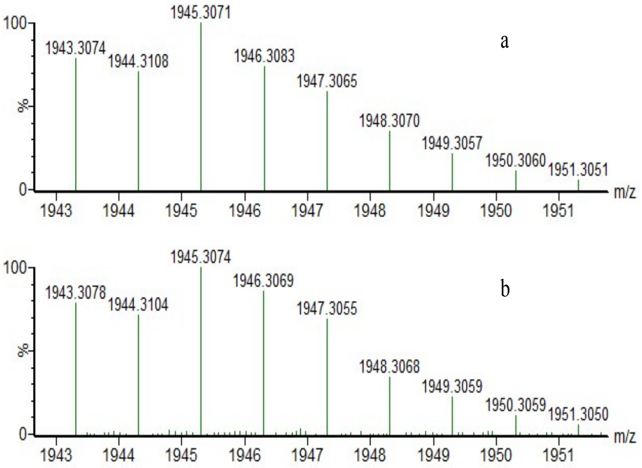

Supplementary Fig. S8-6. Theoretical isotopic distribution (a) and measured isotopic distribution (b) of $C_{81}H_{87}O_{48}Ni_2$

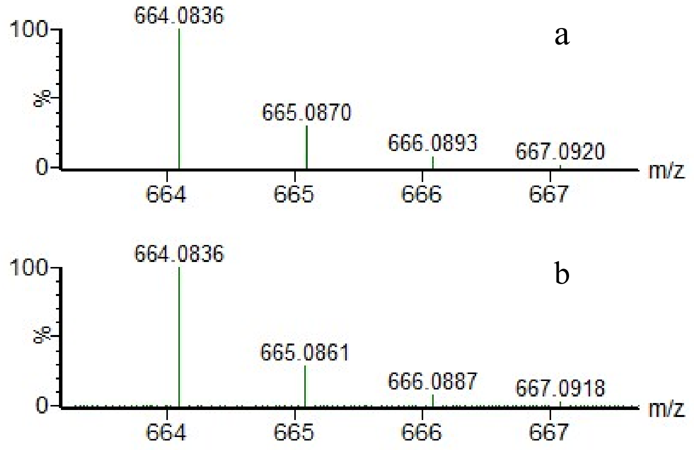

Supplementary Fig. S9-1. Theoretical isotopic distribution (a) and measured isotopic distribution (b) of $C_{27}H_{29}O_{16}Mn$

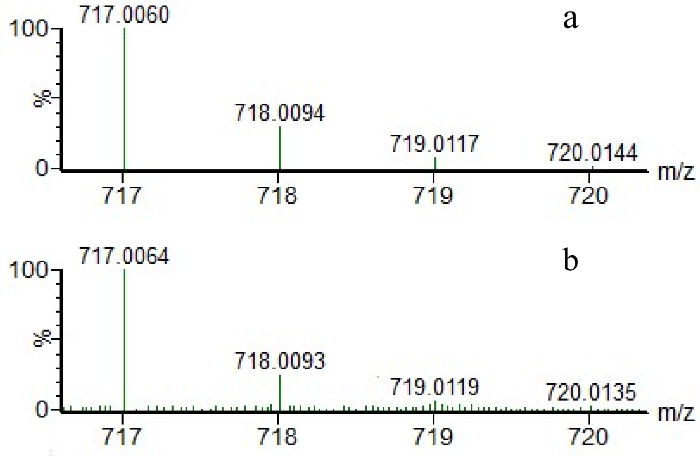

Supplementary Fig. S9-2. Theoretical isotopic distribution (a) and measured isotopic distribution (b) of $C_{27}H_{27}O_{16}Mn_2$

Supplementary Fig. S9-3. Theoretical isotopic distribution (a) and measured isotopic distribution (b) of $C_{54}H_{59}O_{32}Mn$

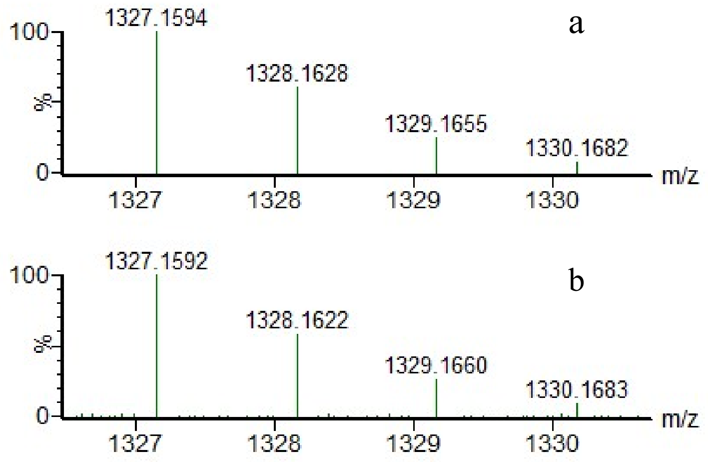

Supplementary Fig. S9-4. Theoretical isotopic distribution (a) and measured isotopic distribution (b) of $C_{54}H_{57}O_{32}Mn_2$

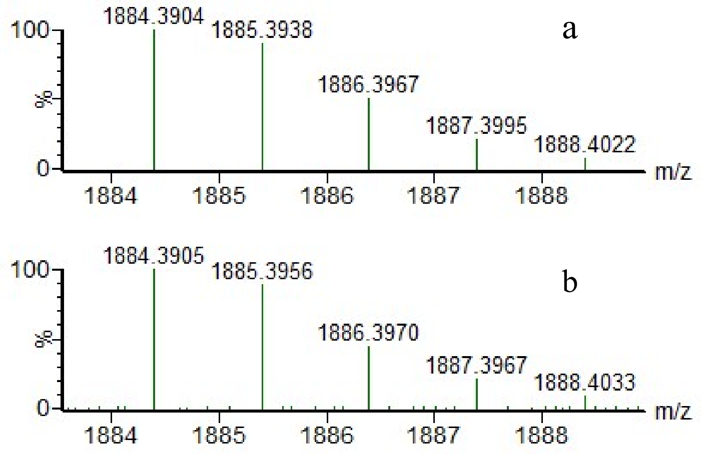

Supplementary Fig. S9-5. Theoretical isotopic distribution (a) and measured isotopic distribution (b) of $C_{81}H_{89}O_{48}Mn$

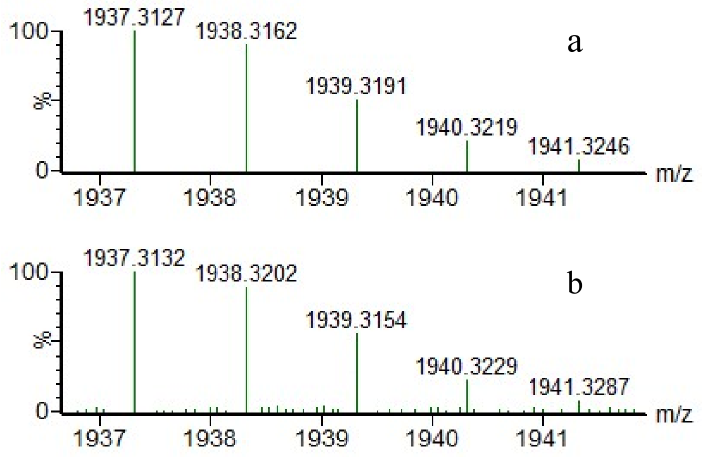

Supplementary Fig. S9-6. Theoretical isotopic distribution (a) and measured isotopic distribution (b) of $C_{81}H_{87}O_{48}Mn_2$

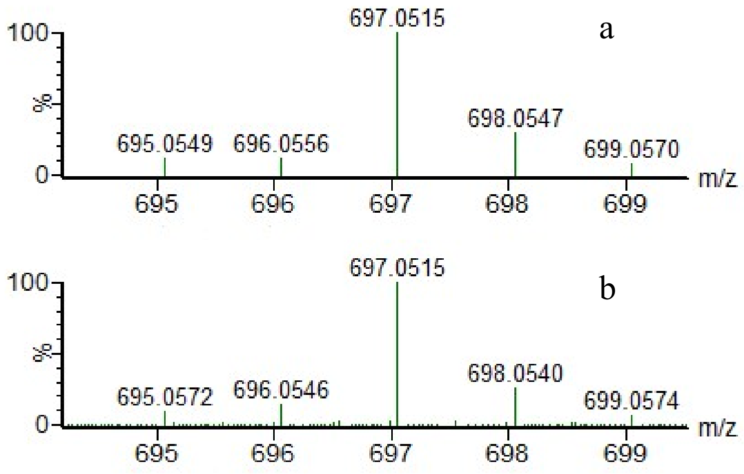

Supplementary Fig. S10-1. Theoretical isotopic distribution (a) and measured isotopic distribution (b) of $C_{27}H_{29}O_{16}Sr$

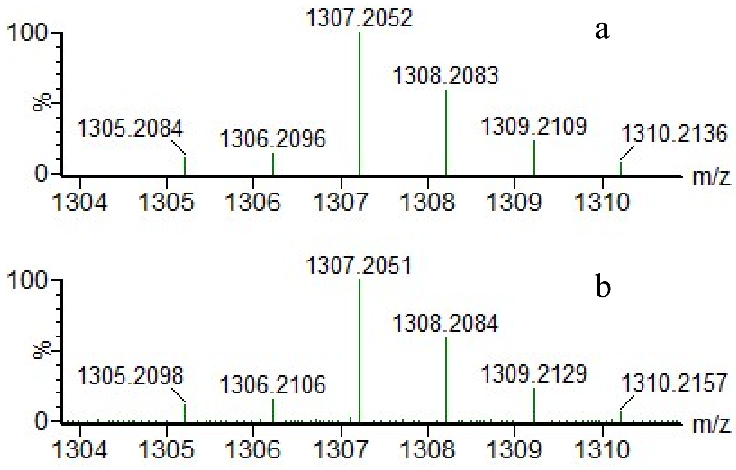

Supplementary Fig. S10-2. Theoretical isotopic distribution (a) and measured isotopic distribution (b) of $C_{54}H_{59}O_{32}Sr$

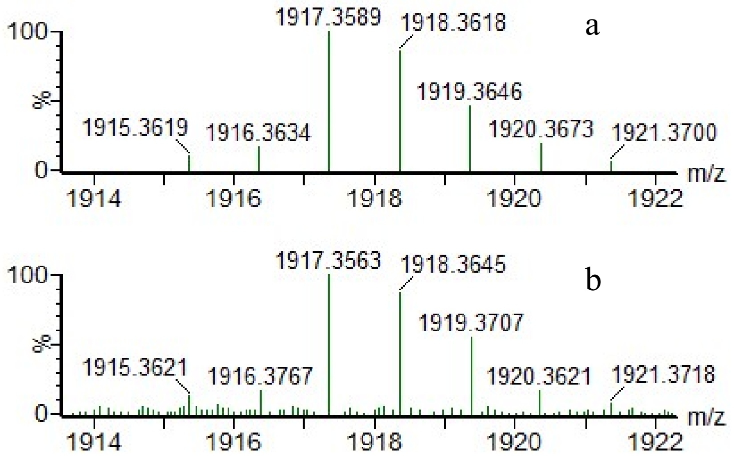

Supplementary Fig. S10-3. Theoretical isotopic distribution (a) and measured isotopic distribution (b) of $C_{81}H_{89}O_{48}Sr$

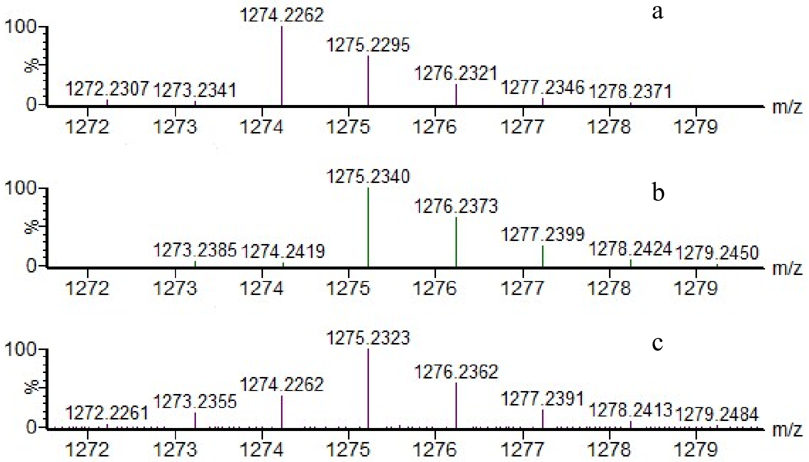

Supplementary Fig. S11-1. Theoretical isotopic distribution of $C_{54}H_{58}O_{32}Fe$（III）(a) and theoretical isotopic distribution (b) and measured theoretical isotopic distribution (c) of $C_{54}H_{59}O_{32}Fe$（II）

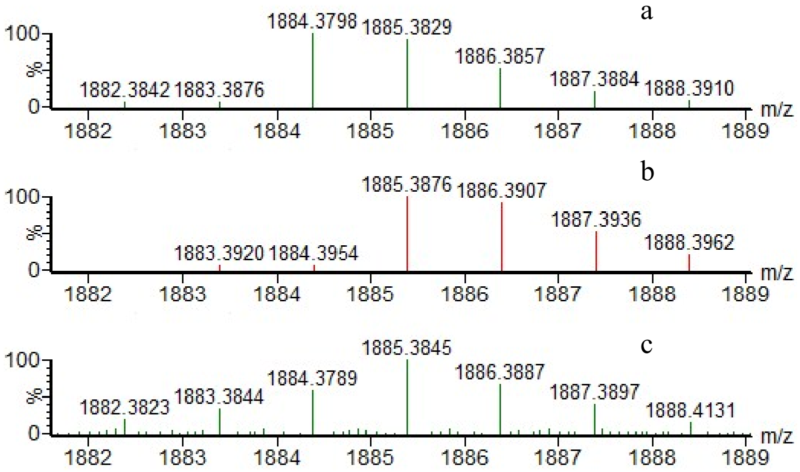

Supplementary Fig. S11-2. Theoretical isotopic distribution of $C_{81}H_{88}O_{48}Fe$（III）(a) and theoretical isotopic distribution (b) and measured theoretical isotopic distribution (c) of $C_{81}H_{89}O_{48}Fe$（II）

Supplementary Table S5. Contents of eight trace elements in aqueous extracts of four medicinal plants and that dissolved in 15 % formic acid-methanol or methanol (μg/g)

	Sophorae Flos			Lonicerae Japonicae Flos			Forsythiae Fructus			Violae Herba		
	Aqueous extract	Methanol	15 % Formic acid-methanol	Aqueous extract	Methanol	15 % Formic acid-methanol	Aqueous extract	Methanol	15 % Formic acid-methanol	Aqueous extract	Methanol	15 % Formic acid-methanol
calcium	115.73 ± 9.26	90.27 ± 7.22	111.38 ± 5.56	1406.8 ± 112.54	1223.92 ± 97.91	1375.55 ± 75.35	528.93 ± 42.31	467.07 ± 31.05	514.17 ± 27.82	4095.43 ± 327.63	3107.75 ± 232.62	3862.67 ± 211.24
magnesium	375.42 ± 30.03	304.09 ± 24.33	369.04 ± 20.15	873.57 ± 69.89	733.8 ± 58.7	861.95 ± 49.52	379.94 ± 30.4	342.34 ± 29.79	368.80 ± 21.54	617.96 ± 49.44	457.29 ± 36.58	603.64 ± 34.89
zinc	19.22 ± 1.54	16.91 ± 1.35	18.48 ± 1.39	10.55 ± 0.84	9.71 ± 0.78	9.52 ± 0.64	15.17 ± 1.21	14.41 ± 1.15	15.11 ± 0.86	9.69 ± 0.77	7.85 ± 0.63	9.26 ± 0.55
iron	73.31 ± 5.87	31.53 ± 2.52	64.08 ± 3.64	229.63 ± 18.37	105.63 ± 8.45	206.44 ± 11.74	51.01 ± 4.08	32.32 ± 3.31	46.62 ± 2.65	86.38 ± 6.91	34.55 ± 2.76	73.17 ± 4.16
copper	2.58 ± 0.21	1.39 ± 0.11	1.99 ± 0.17	2.00 ± 0.16	1.10 ± 0.09	1.65 ± 0.09	0.96 ± 0.08	0.73 ± 0.06	0.85 ± 0.05	1.40 ± 0.11	0.68 ± 0.05	1.12 ± 0.06
nicke	4.04 ± 0.32	2.79 ± 0.22	3.90 ± 0.24	3.98 ± 0.32	2.86 ± 0.23	3.88 ± 0.27	4.17 ± 0.33	3.49 ± 0.29	4.08 ± 0.33	3.47 ± 0.28	2.36 ± 0.19	3.17 ± 0.18
manganese	5.57 ± 0.45	4.01 ± 0.32	5.52 ± 0.31	8.87 ± 0.71	6.83 ± 0.55	8.37 ± 0.49	5.68 ± 0.45	5.17 ± 0.41	5.49 ± 0.31	15.86 ± 1.27	10.47 ± 0.84	14.81 ± 0.84
strontium	1.41 ± 0.11	1.08 ± 0.09	1.38 ± 0.08	0.49 ± 0.04	0.39 ± 0.03	0.45 ± 0.03	0.70 ± 0.06	0.57 ± 0.04	0.68 ± 0.04	2.28 ± 0.17	1.48 ± 0.11	2.14 ± 0.28

Values are given as the mean ± standard deviation, n = 3

10 g of each dried medicinal plant powder were soaked in 150 mL of ultrapure water for 30 min at 25 °C. Reflux extraction was then performed at 100 °C for 3 h, followed by vacuum filtration at 70 °C. The filtrate of each medicinal plant was split into three portions of equal volume, which were separately concentrated to dryness under vacuum to obtain aqueous extracts. Two portions of aqueous extracts were dissolved in 50 mL (10 mL × 5) methanol and 15 % formic acid-methanol solutions separately, centrifuged (10000 × *g*, 10 min), the supernatant to was concentrated to dryness under vacuum and weighed.

Samples were put into polytetrafluoroethylene tubes, followed by the addition of 65% nitric acid (8mL) and 30% hydrogen peroxide (2 mL), and the mixtures were digested in a microwave digestion instrument (MARS5, CEM, USA). The digests were cooled to room temperature, diluted to 50 mL with ultrapure water (contained 0.5% nitric acid), and analyzed by ICP-MS (Agilent 7700, Agilent, USA).

It can be seen from the data in Tables S5–S8 that: 1) all the aqueous extracts of the four medicinal plants contained the eight metal elements used in this paper. However, the content are quite different. The Sophorae Flos aqueous extract contained the highest content of zinc and copper, the Lonicerae Japonicae Flos aqueous extract contained the highest content of magnesium and iron, the Forsythiae Fructus aqueous extract contained the highest content of nickel, the Violae Herba aqueous extract contained the highest content of calcium, manganese, and strontium. 2) Four aqueous extracts contained organic compound-metal complexes, and these complexes cannot be completely dissolved in methanol, but will decompose in 15% formic acid-methanol, resulting in an increase in metal ion content.